Mössbauer-Effect Observations of Recoil Radiation Damage Following Coulomb Excitation in Various Hf Compounds*

C. G. JACOBS, JR.,† AND N. HERSHKOWITZ
Department of Physics and Astronomy, The University of Iowa, Iowa City, Iowa 52240
(Received 25 July 1969)

Mössbauer-effect experiments following Coulomb excitation have been performed involving Hf nuclei in Hf metal, HfB_2 HfC, HfN, and HfO_2. The first excited states of Hf^{178}, Hf^{180}, and Hf^{177} were populated via Coulomb excitation by 6-MeV α particles. The majority of the experiments were performed with both targets and absorbers near liquid-nitrogen temperature. Anomalous hyperfine interactions are found in all of the compounds when they are used as targets, compared to the hyperfine interactions observed when they are used as absorbers. The anomalous interactions are interpreted in terms of lattice distortions resulting from vacancies produced in the locale of the decaying recoil Mössbauer nuclei following Coulomb excitation. The degree of lattice distortion is found to be dependent upon the bonding characteristics of the compounds.

I. INTRODUCTION

RECENTLY, Coulomb excitation and nuclear reactions have become standard techniques used for producing nuclear excitations appropriate for observing the Mössbauer effect of the deexcitation γ rays. During Coulomb excitation or during a nuclear reaction, the excited nucleus recoils out of its lattice site. It is possible that an excited nucleus could create radiation damage in the lattice due to this recoil. The associated Mössbauer effect should be sensitive to such damage. The observation of abnormal hyperfine interactions or reduced recoilless fractions could indicate that the lattice is locally damaged or that the recoil nuclei regularly stop in interstitial positions. Interactions of the lattice with the incident flux, however, can also produce similar effects.

The first observations of the Mössbauer effect following Coulomb excitation were reported by Lee *et al.*[1] and by Seyboth *et al.*[2] An Fe^{57} metal target was bombarded by Lee *et al.* and the Mössbauer effect was observed with a metal absorber. The width and depth of the absorption dips in the resulting spectrum indicated that the difference in the magnetic hyperfine interactions of the target and the absorber was less than 10%. Seyboth *et al.* observed the 67.4-keV transition of Ni^{61} in Ni metal. A 50% broadening of the 35-line envelope was reported when compared to data obtained with a radioactive source. They concluded that the Coulomb-excited nuclei were in an abnormal environment. Decreased recoilless fractions were reported following (n,γ) reactions[3] and (d,p) reactions.[4,5] A neutron-capture experiment by Fink and Kienle indicated that recoil effects from cascade γ rays produced about a 10% increase in the width of the absorption dip when Gd_2O_3 was the target and Gd metal was the absorber, compared to the reciprocal experiment.[6]

Calculations for bcc and fcc lattices indicate that replacement collisions should be a dominant effect in the stopping of energetic particles which have the same mass as the atoms in the crystal.[7–9] A replacement collision occurs when a moving atom strikes an atom located in a lattice, transferring sufficient momentum to the stationary atom to knock it from its lattice site, with the incident atom stopping in the resulting vacancy. These computer "experiments" also indicated that vacancies would be formed in the direct neighborhood of the replacement collision, with the associated interstitial atoms being located several interatomic distances away.

Although these results were for crystal compounds of only one atomic species, calculations for a two-dimensional binary lattice have been done giving a similar result.[10] Such vacancies may be expected to produce distortions which would alter observed Mössbauer spectra. However, an unambiguous example of this effect had not been reported prior to a preliminary publication of the results described here.[11] Reduced recoilless fractions, for example, might be attributed to the emission of γ rays associated with atomic vibrations in the direction of a vacancy, but this could also result from interactions of the lattice with the incident flux.[12] Experiments have been reported in

* Work supported in part by the National Science Foundation.
† NASA trainee. Present address: Pacific Lutheran University, Tacoma, Wash. 98447.
[1] Y. K. Lee, P. W. Keaton Jr., E. T. Ritter, and J. C. Walker, Phys. Rev. Letters **14**, 957 (1965).
[2] D. Seyboth, F. E. Obenshain, and G. Czjzek, Phys. Rev. Letters **14**, 954 (1965).
[3] D. W. Hafemeister and E. Brooks Shera, Phys. Rev. Letters **14**, 593 (1965).
[4] D. A. Goldberg, P. W. Keaton, Jr., Y. K. Lee, L. Madansky, and J. C. Walker, Phys. Rev. Letters **15**, 418 (1965).
[5] S. L. Ruby and R. E. Holland, Phys. Rev. Letters **14**, 591 (1965).
[6] J. Fink and P. Kienle, Phys. Letters **17**, 326 (1965).
[7] J. B. Gibson, A. N. Goland, M. Milgram, and G. H. Vineyard, Phys. Rev. **120**, 1229 (1960).
[8] C. Erginsoy, G. H. Vineyard, and A. Englert, Phys. Rev. **133**, A595 (1964).
[9] C. Erginsoy, G. H. Vineyard, and A. Shimizu, Phys. Rev. **139**, A118 (1965).
[10] J. R. Beeler, Jr., and D. G. Besco, in *Proceeding of a Symposium on Radiation Damage in Solids, Venice 1962* (International Atomic Energy Agency, Vienna, 1962), Vol. 1, p. 43.
[11] C. G. Jacobs, Jr., N. Hershkowitz, and J. B. Jeffries, Phys. Letters **29**, 498A (1969).
[12] G. Czjzek, J. L. C. Ford, Jr., J. C. Love, F. E. Obenshain, and H. H. F. Wegener, Phys. Rev. **174**, 331 (1968).

TABLE I. Percent abundance, energy, and half-life of the first excited state of Hf^{177}, Hf^{178}, and Hf^{180} together with the Coulomb excitation cross section for populating the first excited state by 6-MeV incident α particles.

Nucleus	% abundance[a]	Energy of first excited state (keV) [a]	Half-life of first excited state (nsec) [a]	Coulomb excitation cross section (mb) [b]
Hf^{177}	18.56	112.97	0.5	397
Hf^{178}	27.1	93.2	1.50	123
Hf^{180}	35.22	93.3	1.50	113

[a] Ref. 28.
[b] Calculated for 6-MeV incident α particles using the partial reduced transition probabilities of N. P. Heydenburg and G. M. Temmer [Phys. Rev. **100**, 150 (1955)]. The total reduced transition probabilities were calculated assuming that internal conversion is the only other open channel. The internal conversion coefficients used are given by J. H. Hamilton *et al.* [Nucl. Data 1, 521 (1966)].

which line broadening, and small extra lines have been observed.[13] In these instances, however, such damage can usually be attributed to the interaction of the lattice with the incident flux associated with the production of the excitation. Although a decaying nucleus may have produced lattice damage due to the kinematic recoil accompanying the production of the excited state, this damage has not been uniquely distinguished from that of other origins.

Mössbauer-effect experiments involving radioactive decays populating the first excited states of Hf^{176}, Hf^{178}, and Hf^{180} have been performed by Gerdau *et al.*[14,15] and by Snyder *et al.*[16] The electric quadrupole hyperfine interaction energies were measured for these isotopes in various Hf compounds (including Hf metal, HfB_2, and HfO_2), and the relative quadrupole moments were reported. A broad single absorption line was observed by Jha *et al.* with a HfC absorber and a $Ta^{178}C$ source.[17] The other reported Mössbauer-effect experiments utilizing a radioactive source were performed by Wiedemann *et al.*[18] They observed the Mössbauer effect of Hf^{177} in HfO_2 and Hf metal following the β decay of Lu^{177} in Lu_2O_3 and Lu metal. Electric quadrupole interactions were found in both Hf compounds. Preliminary data obtained following Coulomb excitation obtained with HfO_2 targets and HfC absorbers has been reported by Wilenzick *et al.*[19] and by Hardy *et al.*[20]

[13] See, for example, E. T. Ritter, P. W. Keaton, Jr., Y. K. Lee, R. R. Stevens, Jr., and J. C. Walker, Phys. Rev. **154**, 287 (1967); V. W. Wiedemann, P. Kienle, and F. Stanek, Z. Physik **15**, 7 (1963); P. Hannaford, C. J. Howard, and J. W. G. Wignall, Phys. Letters **19**, 257 (1965).
[14] E. Gerdau, H. J. Körner, J. Lerch, and P. Steiner, Z. Naturforsch. **21a**, 941 (1966).
[15] E. Gerdau, P. Steiner, and D. Steenken, in *Hyperfine Structure and Nuclear Radiations*, edited by E. Matthais and D. A. Shirley (Wiley-Interscience, Inc., New York, 1968), p. 261.
[16] R. E. Snyder, J. W. Ross, and D. St. P. Bunbury, J. Phys. **C1**, 1662 (1968).
[17] S. Jha, W. R. Owens, and B. L. Robinson, Bull. Am. Phys. Soc. **13**, 60 (1968).
[18] V. W. Wiedemann *et al.*, Ref. 13.
[19] R. M. Wilenzick, K. A. Hardy, and D. C. Russell, Bull. Am. Phys. Soc. **13**, 690 (1968).
[20] K. A. Hardy, R. M. Wilenzick, and J. A. Hicks, Bull. Am. Phys. Soc. **14**, 133 (1969).

In this paper, we report observations of the Mössbauer effect following Coulomb excitation of Hf^{177}, Hf^{178}, and Hf^{180} nuclei in Hf metal, HfB_2, HfC, HfN, and HfO_2. Anomalous hyperfine interactions are found in all of the compounds when they are used as targets, compared to the hyperfine interactions observed when they are used as absorbers.

II. TARGET AND ABSORBER MATERIALS

The isotopes of Hf with masses 177, 178, and 180 are appropriate nuclei for Coulomb excitation Mössbauer-effect experiments in that they have $E2$ transitions to their first excited states of energies near 100 keV and are all relatively abundant. Table I lists the excitation energies and lifetimes of the first excited states, the natural abundances of these isotopes, and the total cross section for Coulomb excitation of each isotope with 6-MeV α particles. Furthermore, Hf forms some of the most refractory compounds known, with the melting point of HfC quoted as $(3928\pm20)°C$.[21] Such high melting points indicate high Debye temperatures and the possibility of observing a Mössbauer effect at liquid-nitrogen temperature, even with transition energies near 100 keV. Hafnium metal, HfB_2, HfC, HfN, and HfO_2 were chosen as the chemical forms to be used, since (a) they represent a logical progression through the Periodic Table, (b) they are probably nonmagnetic, at 78°K, (c) they all melt above 2200°C, and (d) they are all readily available.

As a check on the crystal structure and the stoichiometry of the powdered compounds used in these experiments, Debye-Scherrer x-ray patterns were taken of each sample. Since HfC has cubic symmetry, two enriched samples of HfO_2 were converted into HfC. Details of the conversion are given elsewhere.[22] Table II lists the crystal-structure type, the measured and the accepted lattice parameter values, and the supplier of each sample. It should be pointed out that the accepted value of 4.6402 ± 0.0005 Å for HfC has been extrapolated to 0% Zr content from data containing as much as 4% Zr atomic composition. The enriched samples contain no Zr; however, slight traces of oxygen could be present. Nonetheless, group-IV carbides are characterized by a wide scatter of quoted lattice parameter values, and it is believed that the samples prepared here are very pure and stoichiometric. Table II also includes the lattice value obtained for HfC at about 90°K and the value measured for an irradiated $Hf^{180}C$ sample. The $Hf^{180}C$ sample has been irradiated with 6-MeV α particles to a total integrated flux of 2.7×10^{18} particles/cm^2. No structural changes were observed in either case apart from a thermal contraction of the sample near 90°K.

[21] E. K. Storms, *The Refractory Carbides* (Academic Press Inc., New York, 1967).
[22] C. G. Jacobs, Jr., Ph.D. thesis, University of Iowa, 1969 (unpublished).

TABLE II. Measured and accepted lattice parameter values, together with the suppliers, of the Hf compounds used in these experiments.

Compound	Measured lattice parameters[a]	Accepted lattice parameters	Supplier
HfB_2	$a=3.1390\pm0.0003$	$a=3.14$ Å [b]	Semielements[c]
	$c=3.4725\pm0.0006$	$c=3.47$ Å	
HfC	$a=4.6423\pm0.0002$	4.6402 ± 0.0005 Å [d]	A. D. McKay[e]
HfC (90°K)	$a=4.6382\pm0.0004$	4.6402 ± 0.0005 Å	A. D. McKay
$Hf^{178}C$	$a=4.6390\pm0.0002$	4.6402 ± 0.0005 Å	Homemade
$Hf^{180}C$	$a=4.6383\pm0.0002$	4.6402 ± 0.0005 Å	Homemade
$Hf^{180}C$	$a=4.6383\pm0.0002$	4.6402 ± 0.0005 Å	Homemade
$Hf^{180}C$ (irradiated)	$a=4.6379\pm0.0003$	4.6402 ± 0.0005 Å	Homemade
HfN	$a=4.5259\pm0.0003$	4.52 ± 0.02 Å [b]	Semielements
		$a=5.11$ Å	
HfO_2	[f]	$b=5.14$ Å $B=99.733°$ [g]	Wah Chung Corp.[h]
		$c=5.28$ Å	

[a] X-ray wavelength used to obtain these values are from J. A. Bearden, Rev. Mod. Phys. 39, 78 (1967).
[b] F. W. Glasser, D. Moshowitz, and B. Post, J. Metals 5, 1119 (1953).
[c] Semi Metals, Inc., Saxonburg, Pa. 16056.
[d] Reference 21.
[e] A. D. McKay, Inc., New York, N. Y. 10038.
[f] Data were consistent with the accepted structure and lattice parameter values. No attempt was made, however, to extract lattice parameter values from these data.
[g] C. E. Curtis, L. M. Doney, and J. R. Johnson, J. Am. Ceram. Soc. 37, 458 (1954).
[h] Wah Chung Corp., Albany, Ore. 97321.

III. EXPERIMENTAL CONDITIONS

A. Experimental Apparatus

Since the energies of the first excited states of the various Hf isotopes are all near 100 keV, it was necessary to cool both the target and the absorber to near or below liquid-nitrogen temperature in order to observe an appreciable Mössbauer effect. The Mössbauer spectrometer which was used in these experiments is shown schematically in Fig. 1 as attached to the Dewar used to maintain the cooling. No mechanical vibrations associated with the Van de Graaff operation or other activities in the room were detectable in the spectrometer. The entire system was evacuated to a pressure of about 1×10^{-5} Torr. A window in the bottom of the target chamber and a hole in the bottom of the thermal-radiation shield made it possible to optically observe the target during an experiment.

The target face made a 45° angle with both the detector and the beam axes. This angle was chosen since (a) the γ rays of relevance to the present Mössbauer-effect experiments are emitted isotropically, (b) it allowed for maximum exposure of the target face to both the beam and the detector, and (c) it allowed for the most convenient design of the spectrometer. The targets were mounted on the end of the copper cold-finger with two machine screws, which made them easily interchangeable.

The absorbers were mounted on a copper plate which was suspended from the bottom of the center well of the Dewar by ten 0.005-in. copper foils. It was possible with this configuration to change absorbers without disturbing the alignment of the drive-rod.

All interfaces which were mechanically connected were coated with thermal compound[23] if they were along thermal-conduction paths. Measurements made with copper-constantan thermocouples located at the center and at the edge of the absorber material showed that the temperature at these points was within 1° of 77.3°K.

The Hf target compounds were mixed in powder form with Armstrong C-7 low-temperature Epoxy resin (with activator "V")[24] in a ratio of about two parts target material to one part Epoxy resin by weight. The absorber materials were also mixed in powder form with Armstrong C-7 Epoxy resin (with activator "V") and were subsequently applied to a soft aluminum holder. A layer of Stycast 2850FT high thermal-conductivity Epoxy resin (with activator "24LV")[25] was applied to improve the thermal conduction across the absorber. Typically, an absorber would contain about 200 mg/cm² of Al, between about 50–200 mg/cm² of absorber material and about 800 mg/cm² of Stycast.

Deexcitation γ rays from the Hf nuclei were detected with a $\frac{1}{8}$-in.-thick NaI(Tl) detector. The resolution of the detector was measured to be 11.7% at 88 keV. The data were accumulated in a Nuclear Data Series 2200 multichannel analyzer having a four-input "multi-scaling" ability, operated in the time mode.[26] One of the 256-channel memory quadrants of the multichannel analyzer was used for the accumulation of a Fe^{57} Mössbauer-effect spectrum used as a velocity calibration.

The absorber was driven in the so-called "constant

[23] Manufactured by Wakefield Engineering, Inc., Delta Division, Wakefield, Mass.
[24] Manufactured by Armstrong Products Co., Inc., Warsaw, Ind.
[25] Manufactured by Emerson and Cuming, Inc., Dielectric Materials Div., Canton, Mass.
[26] Manufactured by Nuclear Data, Inc., Palatine, Ill.

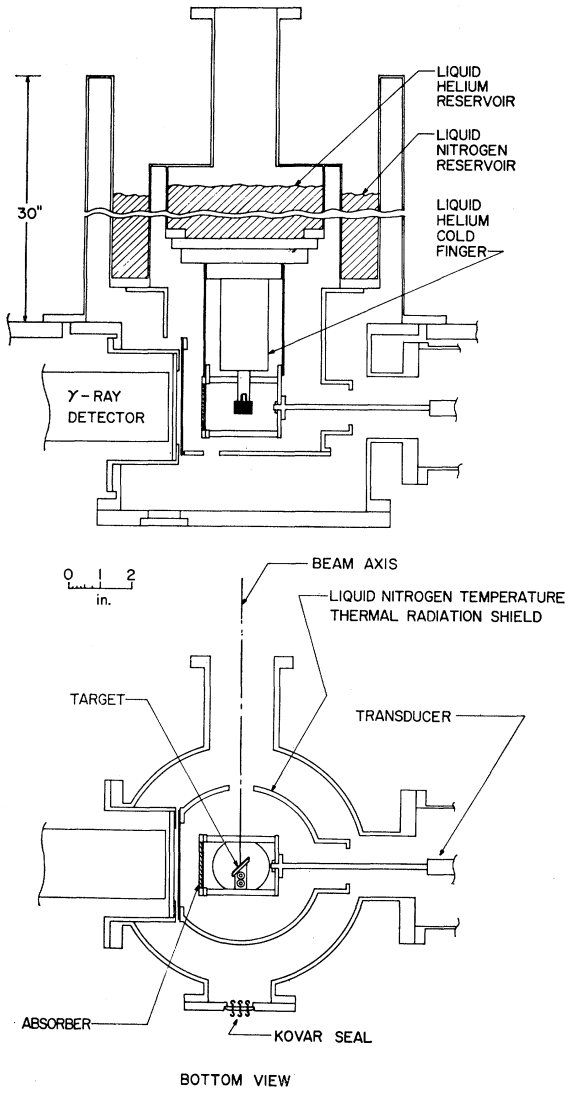

FIG. 1. Schematic representation of a "cut-away" view of the Mössbauer cryostat system.

acceleration mode" by the transducer shown in Fig. 2. The electronic equipment associated with the drive is essentially that described by Cohen *et al.*[27] The dc drifts were always kept less than 0.5% of the maximum drive amplitude, and the ac error usually was less than 0.8% of the desired velocity.

B. Choice of Bombarding Particle

A number of factors led to the choice of He^4 ions for the bombarding particles: (a) Although in the present experiments one expects a drop of about 50% in total γ-ray yield in choosing 6-MeV α particles instead of 6-MeV protons, it was found that the signal-to-noise ratio was improved with α particles to the extent that there was a net gain in the quality of the data obtained per hour of data accumulation. The difference is a consequence of the different rates at which the protons and α particles produced the 56-keV Hf K x ray. The ratio of K x-ray to γ-ray production changed from 55.9:1 for protons on Hf metal to 3.77:1 for α particles. (b) α particles are also advantageous in that He is chemically inert and large irradiation doses should not change the chemical composition of the target. Furthermore, He nuclei have no bound excited states, with the first break-up threshold being at about 20-MeV excitation, eliminating possible γ-ray background problems which might arise due to an accumulation of the bombarding particle in the target material. (c) The use of protons for the bombarding particle was also discouraged by the $Cu^{65}(p,n)Zn^{65}$ reaction. Cryogenic considerations required that large amounts of Cu be present in the target chamber. Since Cu^{65} constitutes 30.9% of natural Cu, this reaction produced high neutron fluxes and γ-ray transitions in Zn^{65} of 54, 61, and 115 keV.[28]

Figure 3(a) shows a typical γ-ray spectrum observed with a 6-MeV α beam incident on a Hf metal target. The spectra in Figs. 3(b) and 3(c) are typical of those observed with targets made with natural and isotopically enriched Hf powders, respectively. Count rates of 1500 counts/sec were regularly obtained with 1 μA of beam on a powder target and the single-channel analyzer window set on the 93-keV line. With a metal target, 4500 counts/sec were obtained with 750 nA of beam. The count rate in the window of one of the single-channel analyzers and the beam at the chamber were periodically checked for consistency throughout an experiment to be sure that no major changes occurred in the beam profile. The He^4 ion beam was adjusted for maximum production of γ rays, while maintaining a diffused beam shape comparable to the target. No target glowing was noted.

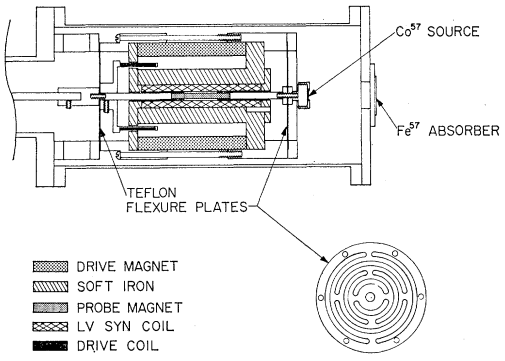

FIG. 2. Schematic representation of a "cut-away" view of the Mössbauer drive transducer.

[27] R. L. Cohen, P. G. McMullin, and G. K. Wertheim, Rev. Sci. Instr. 34, 671 (1963).

[28] C. M. Lederer, J. M. Hollander, and I. Perlman, *Table of Isotopes* (John Wiley & Sons, Inc., New York, 1967).

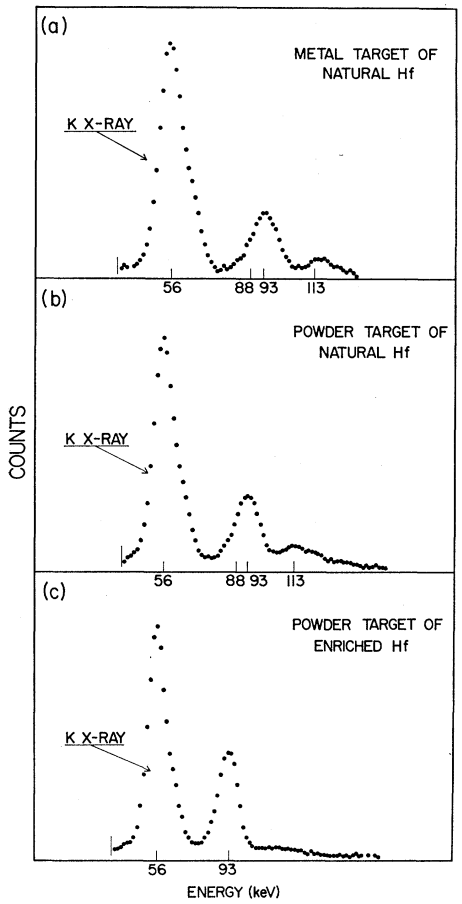

FIG. 3. Pulse-height spectra obtained by bombarding (a) a natural metal target, (b) a natural powder target, and (c) an isotopically enriched powder target with 6-MeV α particles.

IV. EXPERIMENTAL RESULTS

A. General Overview of Results

Mössbauer spectra were obtained for various target and absorber combinations of Hf metal, HfB_2, HfC, HfN, and HfO_2. In two of the experiments the Mössbauer effect of the 113-keV transitions in Hf^{177} was observed. The remainder of the experiments involved the Mössbauer effect of the 93-keV transitions in Hf^{178} and Hf^{180}. Two of these experiments were performed with enriched HfC targets at a temperature of about 50°K and a HfO_2 absorber at about 15°K. All others were performed with the target and absorber temperatures within 1°K of liquid-nitrogen temperature. No differences could be observed in the Mössbauer spectra obtained with 4.5- and 6.0-MeV incident α-particle energies.

The observed shapes of the Mössbauer spectra remained unchanged during the course of an experiment. Figure 4 shows the area of the absorption dip as a function of the data acquisition time for two sets of HfC-target data. These represent a part of the data

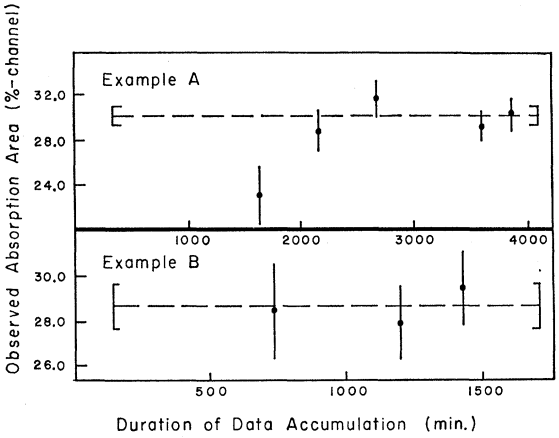

FIG. 4. Plots of the area of the Mössbauer absorption dip as a function of the total time of data acquisition for two sets of HfC target. The dashed line represents the weighted average value.

added together to give the results shown in Fig. 5 (a). The first data point plotted in example A on Fig. 4 is low owing to a higher heat input on the target during this period. Although the shape of the Mössbauer spectrum did not differ at this point in the experiment from that corresponding to the other points, the per-

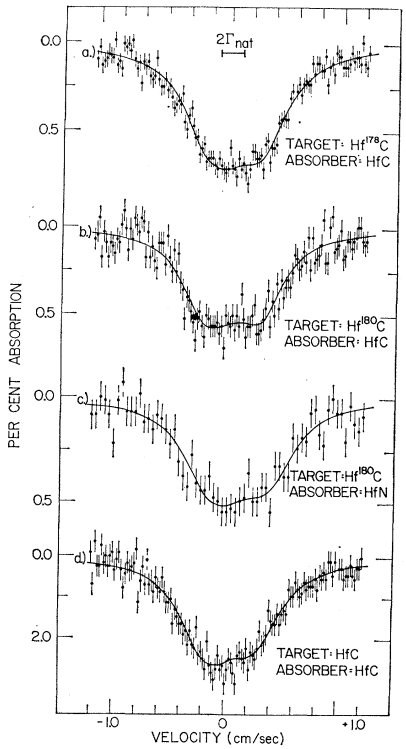

FIG. 5. Mössbauer absorption spectra obtained with HfC targets and HfC absorbers together with the corresponding plots of the fitted curves obtained assuming that electric quadrupole hyperfine interactions were present only in the targets. The respective absorber thicknesses in mg/cm² are (a) 77, (b) 77, (c) 73, and (d) 204 of natural Hf.

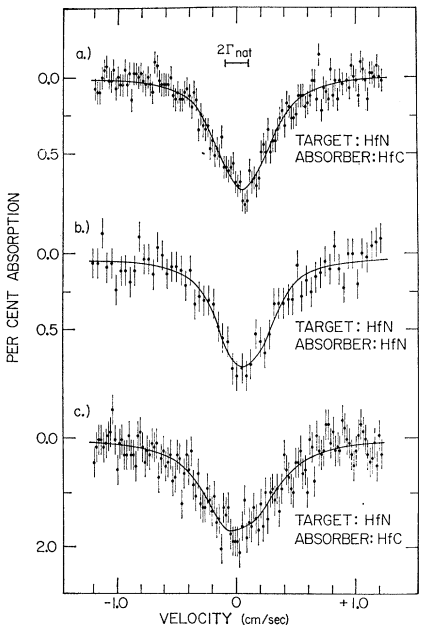

FIG. 6. Mössbauer absorption spectra obtained with a HfN target and HfN or HfC absorbers, together with the corresponding plots of the fitted curves obtained assuming that electrical quadrupole hyperfine interactions were present only in the target. The respective thicknesses in mg/cm² are (a) 77, (b) 73, and (c) 204 of natural Hf.

cent absorption was reduced by a 30% higher beam current during this period than in the remainder of the time. It was found that with HfO_2 targets an acceptable effect could be observed with 500 nA on target, but that no effect could be seen with 2 μA. This is attributed to gross lattice heating.

The total number of particles incident on a lattice during any of these experiments never exceeded 1.8% of the total number of target atoms, the result for five days of running. The shape of a Mössbauer spectrum remained unchanged throughout the course of an experiment from the time it was first discernible, usually after about 3–4 h. No change was observed in the Debye-Scherrer x-ray powder pattern of a HfC target after an integrated irradiation of 2.7×10^{18} α particles/cm² when compared to the pattern taken of the same material prior to irradiation.

TABLE III. FWHM of the Mössbauer absorption dips for various HfC and HfN target-absorber combinations.

Target	Absorber	Natural thickness (mg/cm²)	Envelope width (mm/sec)
$Hf^{178}C$	HfC	77	9.30±0.38
$Hf^{180}C$	HfC	77	9.52±0.39
$Hf^{180}C$	HfC	204	9.52±0.39
$Hf^{180}C$	HfN	73	9.69±0.39
HfC	HfC	204	8.97±0.39
	Weighted average =		9.40±0.17
HfN	HfN	73	5.03±0.39
HfN	HfC	77	5.41±0.39
HfN	HfC	204	6.63±0.39
	Weighted average =		5.69±0.23

TABLE IV. Relative isomer shifts, electric-field-gradient asymmetry parameter values, and the hyperfine interactions energies observed for various HfC and HfN target-absorber combinations.

Target	Absorber	Natural thickness (mg/cm²)	Relative isomer shift (mm/sec)	η	$\frac{1}{4}eQV_{zz}$ (mm/sec)
$Hf^{178}C$	HfC	77	0.34±0.06	0.80±0.16	−2.37±0.10
$Hf^{180}C$	HfC	77	0.23±0.10	0.82±0.20	−2.51±0.14
$Hf^{180}C$	HfC	204	0±0.19	0.60±0.30	−2.29±0.21
$Hf^{180}C$	HfN	73	0.35±0.17	0.68±0.43	−2.53±0.26
HfC	HfC	204	0.35±0.08	0.61±0.23	−2.42±0.12
	Weighted average =		0.31±0.04	0.74±0.10	−2.41±0.06
HfN	HfN	73	0.19±0.12	defined = 0	−1.30±0.21
HfN	HfC	77	0.08±0.08	defined = 0	−1.30±0.23
HfN	HfC	204	0.22±0.14	defined = 0	−1.71±0.23
	Weighted average =		0.13±0.06		−1.43±0.13

B. Results Involving HfC and HfN Target-Absorber Combinations

All of the Mössbauer spectra obtained following the Coulomb excitation of the Hf nuclei exhibited anomalous characteristics. However, the most evident anomalies are found in those spectra involving HfC and HfN targets. Both of these compounds are cubic and nonmagnetic, and, therefore, they should produce no hyperfine interactions. Yet the Mössbauer spectra involving these compounds as both the target and the absorber had envelope widths [the full width at half-maximum (FWHM) of the Mössbauer absorption dips] which were grossly different from the expected value of twice natural linewidth, i.e., $2\Gamma_{nat}$. Table III lists the envelope widths of the observed spectra for those compounds. If 1.50 nsec is taken to be the half-life of the first excited state in Hf^{178} and Hf^{180}, $2\Gamma_{nat}=1.95$ mm/sec.[28] It is significant that the envelope width does not depend on whether HfC or HfN is the absorber, indicating that the hyperfine interactions are the same in both compounds when used as absorbers. On the basis of the envelope width observed with the HfN target, it is concluded that the absorber hyperfine interaction energies are less than $\frac{1}{2}\times(5.22)$ mm/sec $=2.61$ mm/sec. This, together with the observed envelope width with the HfC targets suggests that the envelope widths are entirely due to anomalies produced in the targets.

Assuming this interpretation, these spectra were fitted with a curve corresponding to electric quadrupole hyperfine interactions in the target and no hyperfine interaction in the absorber. The relative positions and depths of the Mössbauer absorption lines were all constrained to be equal. Table IV lists the results of these fits, and Figs. 5 and 6 show the data together with the fitted curves for the HfC and HfN target data, respectively. The weighted average FWHM of the hyperfine Mössbauer lines is $(2.58\pm0.2)\times2\Gamma_{nat}$ with the HfC targets and $(2.09\pm0.17)\times2\Gamma_{nat}$ with the HfN

target. All uncertainties quoted are standard deviations obtained from the fitting routine.

In all cases, satisfactory fits to the HfN target data could be made without letting the asymmetry parameter vary, and it was defined to be zero. Although these data do not allow an unambiguous determination of the sign of the interaction energy, its magnitude and the other fitted parameters are not affected by a change in the sign. The negative sign has been listed as the result of a visual evaluation of the corresponding fits.

In an attempt to explain the widths required for satisfactory fits to all of these data, an additional experiment was performed so that a comparison of the absorption areas could be made for two different absorber thicknesses. One disadvantage of using Coulomb excitation in conjunction with Mössbauer-effect experiments is that recoilless fraction measurements are extremely difficult to make. The spectrum shown in Fig. 8(a) represents a total of eight days of data acquisition. Fluctuations the order of 10% occurred in the beam current. Such fluctuations resulted in large uncertainties in the absorption area, as shown in Fig. 7. The experimental conditions of this experiment were reproduced, but with a 204-mg/cm²-thick absorber. It was not feasible to use an absorber thickness thinner than 77 mg/cm² since this would entail too long a data acquisition period. The area ratio $A(204)/A(77)$ equaled 1.81 ± 0.12. It was therefore concluded that the required widths could not be explained in terms of absorber broadening since the ratio corresponded to $t=2.2_{-0.4}{}^{+2.8}$, or a Debye temperature $\Theta_D=320_{-30}{}^{+120}$ °K. Debye temperatures of (176 ± 10)°K and (226 ± 10)°K have been reported by Wiedemann *et al.*[18] for Hf metal and HfO_2, respectively, so a Debye temperature near 300°K for HfC is not unreasonable considering the relative melting temperature of these compounds. Assuming a Debye temperature of 300°K, the recoilless fraction for both the target and the absorber is calculated to be $f\simeq0.12$, which agrees with the observed HfC spectra.

A Mössbauer effect following Coulomb excitation of the 113-keV level of Hf^{177} was observed. The target was composed of natural HfC and the absorber was 204 mg/cm² of HfC. The area of the absorption dip was measured to be $(2.89\pm0.69)\%$ mm/sec.

C. Results Involving HfO_2

Two experiments were performed in which the Mössbauer effect was observed following the Coulomb excitation of Hf^{178} and Hf^{180} nuclei located in HfO_2. The data obtained in these two experiments were fitted assuming electric quadrupole hyperfine interactions in the target material, and no hyperfine interactions in the HfC absorber. Table V lists the results of these fits, and Figs. 7(a) and 7(b) show plots of these fits with the corresponding data. A FWHM of the Mössbauer hyperfine lines equal to $(2.42\pm0.25)\times2\Gamma_{nat}$ was required for these fits. The electric-field-gradient asymmetry parameter was defined to be zero in these fits, and the relative positions and intensities were constrained according to theory.

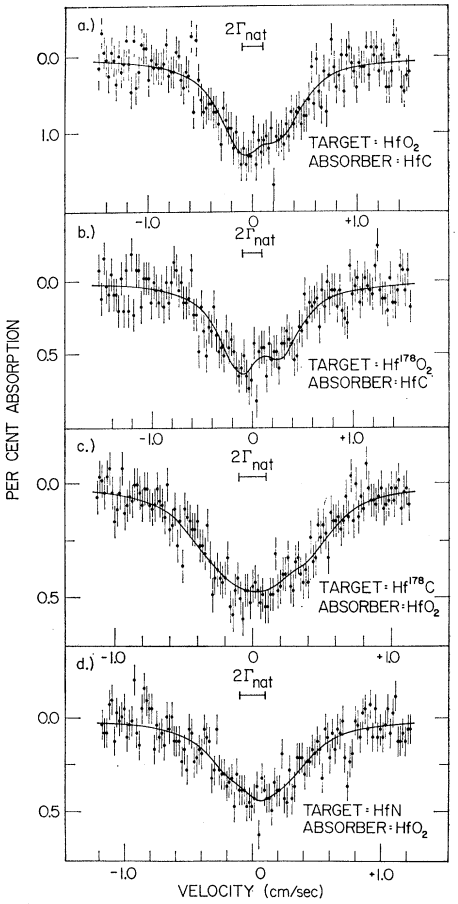

FIG. 7. Mössbauer absorption spectra obtained with HfO_2 as either the target or the absorber, together with the fitted curves. These curves in (a) and (b) were obtained assuming that electric quadrupole hyperfine interactions were present only in the targets. The curves in (c) and (d) were obtained by constraining the target hyperfine interactions to be those obtained with a HfC or HfN absorber and assuming that electric quadrupole interactions were present in the absorber. The respective absorber thicknesses in mg/cm² are (a) 77, (b) 77, (c) 73, and (d) 73 of natural Hf.

The weighted average hyperfine interaction energy obtained in the present set of experiments is about 25% larger than the values reported by Gerdau *et al.*[14,15]

TABLE V. Relative isomer shifts and the hyperfine interaction energies observed with a HfC absorber and $Hf^{178}O_2$ and HfO_2 targets.

Target	Absorber	Natural thickness (mg/cm²)	Relative isomer shift (mm/sec)	$\frac{1}{4}eQV_{zz}$ (mm/sec)
$Hf^{178}O_2$	HfC	77	0.38 ± 0.17	-2.60 ± 0.18
HfO_2	HfC	77	0.42 ± 0.16	-2.32 ± 0.21
Weighted averages=			0.40 ± 0.12	-2.48 ± 0.1

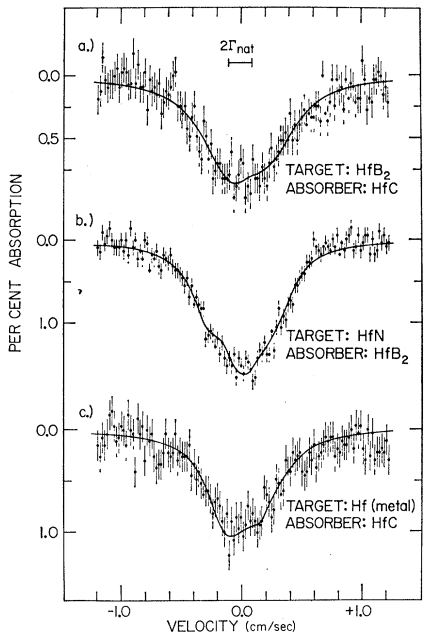

FIG. 8. Mössbauer absorption spectra obtained with (a) a HfB_2 target, (b) a HfB_2 absorber, and (c) a Hf metal target, together with the fitted curves. These curves in (a) and (c) were obtained assuming electric quadrupole interactions were present only in the targets. The curve in (b) was obtained by constraining the target hyperfine interactions to be those obtained with the a HfC or HfN absorber and assuming that electric quadrupole interactions were present in the absorber. The respective absorber thicknesses in mg/cm² are (a) 77, (b) 73, and (c) 204 of natural Hf.

and Snyder *et al.*[16] In order to ascertain whether this discrepancy indicated anomalous hyperfine interactions when HfO_2 was used as a target compared to those measured with HfO_2 as an absorber, data from two experiments were fitted in a highly constrained manner. These data involved $Hf^{178}C$ and HfN as the target material and a 71-mg/cm² HfO_2 absorber. The curves fitted to these data were calculated with the target parameters fixed to the values obtained in the HfC and HfN experiments. The absorber hyperfine interaction energy was allowed to vary, with the relative line positions and depths constrained by assuming electric quadrupole interactions. The asymmetry parameter was defined to be zero in the absorber. The results of these two fits are shown in Figs. 7(c) and 7(d). The weighted average hyperfine interaction energy obtained from these fits is $\frac{1}{4}eQV_{zz}=-1.65\pm0.25$ mm/sec, with relative isomer shifts of 0.41 ± 0.14 and 0.53 ± 0.16 mm/sec for the $Hf^{178}C$ target and HfN target data, respectively.

Additional data were taken with enriched $Hf^{178}C$ and $Hf^{180}C$ targets at an estimated temperature of 80°K, with a HfO_2 absorber of 71 mg/cm² at an estimated 110°K. The incident α-particle energy was 4.5 MeV. The values obtained from these fits are completely consistent with those obtained with both the target and absorber near liquid-nitrogen temperature and 6-MeV incident α particles.

D. Results Involving HfB_2

A Mössbauer spectrum was obtained with a HfB_2 target and a 77-mg/cm² HfC absorber. Figure 8(a) shows a plot of the data with the hyperfine lines constrained to represent an electric quadrupole interactions in the target. Since HfB_2 has an hexogonal close-packed crystal structure, the electric field gradient at the Hf nuclei should have no asymmetry. The hyperfine interaction energy extracted in this fit is $\frac{1}{4}eQV_{zz}=-2.10\pm0.16$ mm/sec for Hf^{178} and Hf^{180} nuclei in HfB_2. A relative isomer shift of 0.30 ± 0.11 mm/sec was observed, and the FWHM of the Mössbauer lines required to obtain a satisfactory fit to these data is $(2.67\pm0.31)\times2\Gamma_{nat}$.

A radioactive source Mössbauer-effect measurement of the electric quadrupole interaction energy for Hf^{178} and Hf^{180} nuclei in HfB_2 has been reported by Snyder *et al.*[16] They report values corresponding to $\frac{1}{4}eQV_{zz}=-1.794\pm0.007$ and -1.753 ± 0.029 mm/sec for Hf^{178} and Hf^{180}, respectively. These values are about 16% smaller than that obtained above.

A second experiment involving HfB_2 was performed to see if a different hyperfine interaction energy would be found when the material was used as an absorber. A HfN target was chosen since it represents the narrowest source found of Hf γ rays following Coulomb excitation. The Mössbauer spectrum obtained with a 73-mg/cm² HfB_2 absorber was fitted with the target hyperfine interaction energy fixed to be that obtained with the HfN absorber and the 77-mg/cm² HfC absorber. Figure 8(b) shows this spectrum together with the fitted theoretical curve. The hyperfine interaction energy obtained for the absorber was $\frac{1}{4}eQV_{zz}=-1.98\pm0.08$ mm/sec which is in agreement with that obtained for HfB_2 as a target.

E. Results Involving Hf Metal

A Mössbauer effect was obtained with a Hf metal target and a 204-mg/cm² HfC absorber for both the 93-keV levels in Hf^{178} and Hf^{180}, and the 113-keV level in Hf^{177}. The Mössbauer spectrum of the 113-keV γ rays was not a pronounced enough effect to allow a detailed analysis of its shape. The area of the absorption dip, however, was $(2.95\pm0.65)\%$ mm/sec. A fit was made to the Mössbauer spectrum of the Hf^{178}-Hf^{180} nuclei assuming electric quadrupole interactions in the metal. The electric-field-gradient asymmetry parameter was constrained to be zero and it was assumed that no hyperfine interactions were present in the absorber. Figure 8(c) shows the Mössbauer spectrum, together with the fitted curve. The hyperfine interaction energy required for a satisfactory fit was found to be $\frac{1}{4}eQV_{zz}=-1.68\pm0.13$ mm/sec, with a hyperfine Mössbauer linewidth of $(1.97\pm0.24)\times2\Gamma_{nat}$.

Mössbauer-effect measurements for the electric quadrupole hyperfine interaction energies for Hf^{178} and Hf^{180} nuclei in Hf metal have been made by Snyder *et al.* utilizing radioactive sources.[16] They report values which correspond to $\frac{1}{4}eQV_{zz}=-1.485\pm0.009$ and -1.443 ± 0.050 mm/sec for Hf^{178} and Hf^{180}, respectively. A value corresponding to $\frac{1}{4}eQV_{zz}=-1.41\pm0.02$ mm/sec has been reported by Gerdau *et al.* for the electric quadrupole interaction energy of Hf^{178} in Hf metal.[15] The interaction energy observed following Coulomb excitation is 0.19 ± 0.13 mm/sec greater than the largest of these reported values. Isomer shifts observed in the above experiment are summarized in Table VI.

An additional Mössbauer-effect experiment was performed involving a Hf metal target and absorber. An area of $(1.25\pm0.20)\%$ mm/sec was observed with an incident beam current of 2.2 μA.

V. DISCUSSION

The anomalous hyperfine interactions which have been observed in these experiments are associated with changes in the local environment of the decaying nuclei. Radiation damage resulting from the incident α particles has been ruled out since (a) the total number of particles incident on a lattice never exceeded 1.8% of the total number of target atoms within the range of the incident particles. (b) Most of these incident particles stopped far from the excited nuclei. (c) The shape of a Mössbauer spectrum remained unchanged during the course of an experiment from the time when it was first discernable. This time usually corresponded to an integrated incident flux of only 0.05% of the number of target atoms within the range of the incident particles. (d) Debye-Scherrer x-ray powder patterns of the target compounds taken before and after irradiation showed no differences. (e) The recoilless fraction of the HfC target was found to be equal to that of the HfC absorber. Therefore, it is concluded that the changes are associated with the recoil Hf nuclei. Such changes could be attributed to lattice distortions or atomic excitations.

Atomic excitation has been suggested by Salomon *et al.* to explain a time-dependent hyperfine interaction (lasting several nanoseconds) of Ta^{181} nuclei following the β decay of Hf^{181}.[29] The time differential angular correlation was observed with the Ta nuclei in HfO_2 which is an insulator. Although it is tempting to attribute the observed anomalies to charge state phenomena, this interpretation is contradicted by other evidence. The hyperfine interaction energy found for Hf nuclei in HfO_2 following Coulomb excitation is only 0.85 ± 0.29 mm/sec larger than that found using HfO_2 as an absorber, while increases of 2.41 ± 0.06 and 1.43 ± 0.13 mm/sec are found, respectively, in HfC and HfN which are not insulators.

TABLE VI. Relative isomer shifts observed for the various target-absorber combinations used in these experiments.

Target	Absorber	Relative isomer shift (mm/sec)
Hf metal	HfC	-0.32 ± 0.49
HfB_2	HfC	$+0.30\pm0.11$
HfC	HfC	$+0.31\pm0.04$
HfC	HfN	$+0.35\pm0.17$
HfC	HfO_2	$+0.36\pm0.11$
HfN	HfB_2	0 ± 0.05
HfN	HfC	$+0.11\pm0.07$
HfN	HfN	$+0.19\pm0.12$
HfN	HfO_2	$+0.53\pm0.16$
HfO_2	HfC	$+0.40\pm0.12$

The other possibility is that the lattice symmetry is locally changed by the recoil particle. Calculations have been made by Dederichs *et al.*[30] in which the probability $P(E)$ is determined that an incident atom of energy E will undergo a replacement collision. It was found in these calculations that $P(E)=\ln 2$ for incident energies greater than $2E_d$, where E_d is a threshold energy corresponding to the minimum energy required to remove an atom from its lattice site in an irreversible fashion. In most metals and semiconductors it is usually considered to be about 25 eV. For incident energies between E_d and $2E_d$, $P(E)$ drops rapidly, equaling zero for $E=E_d$. These calculations assumed a completely random distribution of positions for the crystal atoms. The regular arrangement of crystal atoms is known to give rise to correlated collisions.

Computer calculations by Gibson *et al.*[7] followed the chain of events resulting when a copper atom was given an energy of up to 400 eV in a fcc crystal consisting of about 500 Cu atoms, and in a few calculations, involving crystals of about 1000 Cu atoms. The motions and interactions of each atom were followed as the energetic atom was stopped and the corresponding energy and momentum were dissipated throughout the crystal.

The results of 45 calculations are reported in which the energy and direction with respect to the crystal of the initial atom motion were varied. The lattice damage consisted of vacancies and interstitials. Replacement collisions were found to be very numerous, and the regular arrangement of the crystal atoms led to what are called "focusing chains." Focusing chains occur when the momentum of a moving atom lies nearly along a line of atoms. In addition to momentum transfer, focusing chains transfer mass. The interstitial configuration at the end of the chain can be many interatomic distances from the vacancy formed at the beginning of the chain. The general qualitative results of these calculations is that, due to the regular arrangement of the atoms in a crystal, lattice damage resulting from a moderately energetic particle which undergoes a replacement collision will consist mainly of a compact

[29] M. Salomon, L. Boström, T. Lindquist, M. Perez, and M. Zwanziger, Arkiv Fysik **27**, 97 (1964).

[30] P. H. Dederichs, Chr. Lehmann, and W. Wegener, Phys. Status Solidi **8**, 213 (1965).

group of vacancies near the replacement site, and a group of interstitials located many interatomic distances away.

Virtually identical calculations have been done by Erginsoy *et al.*[8,9] for bcc α iron. Focusing chain effects were also found in these calculations. Initial energies varying up to 1500 eV were considered, with the mean number of lattice defects being found to be proportional to the initial energy. For initial energies of up to 1.5 keV, the calculations showed no evidence of channeling. It was concluded that this resulted from the fact that the initially energetic atom always started from a lattice position.

A similar set of calculations has been made by Beeler and Besco for a two-dimensional binary lattice of BeO, with incident I^{127} and Kr^{84} atoms of energies ranging from 1 to 50 keV.[10] The computations were limited to a two-dimensional lattice because programming for a dynamic event in a binary lattice is significantly more complex than in a lattice composed of only one atomic species. When the incident direction was one of low crystal symmetry, results similar to Gibson *et al.* and Erginsoy *et al.* were observed. The general resulting configurations were characterized by a central region with many vacancies and few interstitials, and the peripheral region having many interstitials and few vacancies.

When Hf nuclei are Coulomb excited by 6-MeV α particles, the maximum kinetic energy which can be given to the Hf atom is about 500 keV corresponding to a 180° scattering of the α particle. A Hf atom of such energy would be expected to be ionized as it passed through a crystal, acquiring electrons as it slowed down. Generally speaking, an electron will be stripped away whose orbital velocity is less than the velocity of the atom, while those with greater orbital velocities will adiabatically distort as the atom encounters crystal atoms.[31] Below some minimum energy ionization will stop being the dominant mode of energy loss since the moving atom will be neutral. Above this energy ionization should be the dominant mode of energy loss, since ionization cross sections are larger than atomic scattering cross sections. The recoil Hf atoms are thus usually moving with an energy below about 180 keV when they experience a replacement collision. This interpretation is consistent with the observation of no significant differences in the HfC target hyperfine interaction parameters when bombarded with incident beam energies of 4.5 and 6 MeV.

Although the calculations of Gibson *et al.* and of Erginsoy *et al.* are for close-packed lattices having only one constituent, the results of Beeler and Besco indicate that recoil Hf atoms with energies below 180 keV probably produce lattice damage similar to that described by the Gibson and Erginsoy calculations. Since the kinematics of the process would seem to be insensitive to the relatively small mass differences of B, C, N, and O compared to the Hf mass, the differences in the hyperfine interactions energies observed with the Hf compounds involving these atoms is attributed to chemical differences of the compounds.

Chemical differences could result in different hyperfine interaction energies upon the removal of one of the constituent atoms in at least two ways. First, if the crystal can be characterized as having ionic bonds, the removal of an atom could create a local imbalance. Second, if the crystal is more properly described in terms of covalent bonds, the strong directional properties of these bonds could effect the lattice symmetry even if no charge imbalance results.

It has been pointed out by Rundle[32] that there exists a large class of metal-nonmetal compounds of formula MX which is characterized by (a) a preference for NaCl structure, (b) very high melting points, (c) good electrical conductivity, and (d) brittleness. Hafnium carbide and nitride both belong to this class of compounds. It is argued that the physical properties can be explained in terms of covalent bonds of fractional order. According to Pauling[33] the bond order can be calculated from the bond length with the equation

$$\Delta R \equiv R_n - R_1 = -0.300 \ln n,$$

where n is the bond order, R_n is the interatomic distance of the two atoms involved in the bond, and R_1 is the distance for a bond of order one given by the sum of Pauling's metallic radii for the two atoms. The Hf—Hf interatomic distance in Hf metal is 3.163 Å, while the Hf—Hf distances in HfC and HfN are 3.281 and 3.196 Å, respectively. In the context of Pauling's rule one would therefore conclude that the Hf—Hf bonds are strongest in Hf metal and weakest in HfC. Since the melting temperature is highest for HfC and lowest for Hf metal, Rundle concluded that the Hf—C and Hf—N bonds are responsible for the melting temperature of these compounds.

Guided by the preference for NaCl structure which indicated octahedral bonding, Rundle suggested that six covalent metal—nonmetal bonds could be formed using two hybrid sp orbitals and the two remaining p orbitals, rather than three p orbitals with no hybridization. Since there are six bonds involved, each having a possible two electrons and only six p electrons allowed, no hybridization corresponds to a bond number of $6/12=\frac{1}{2}$. If the two s electrons can participate in the bonding due to hybridization, the bond number thus becomes $8/12=\frac{2}{3}$. Using Pauling's rule, hybridization implies $\Delta R=0.122$ Å, while no hybridization gives $\Delta R=0.208$ Å. The observed ΔR for HfC is 0.107 Å, with $\Delta R=0.122$ Å for HfN. Thus, the metal–nonmetal bonds in both HfC and HfN are probably of order $\frac{2}{3}$.

[31] G. J. Dienes and G. H. Vineyard, *Radiation Effects in Solids* (Wiley-Interscience, Inc., New York, 1957).

[32] R. E. Rundle, Acta Cryst. **1**, 180 (1948).

[33] L. Pauling, J. Am. Chem. Soc. **69**, 542 (1947).

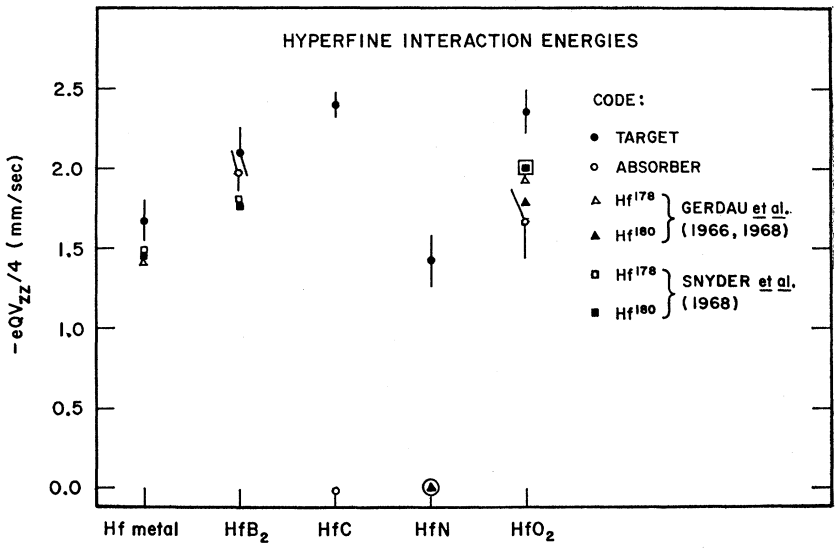

FIG. 9. Graphical comparison of the hyperfine interaction energies as reported in the literature and observed in these experiments for Hf^{178} and Hf^{180} nuclei in Hf metal, HfB_2, HfC, HfN, and HfO_2.

In the context of Rundle's model, the additional electron provided by the nitrogen atom allows an additional electron for the Hf-Hf bonds since the metal-nonmetal bonds are assumed to contain eight electrons in both HfC and HfN. Even though it is assumed that the Hf-Hf bond lengths do not fix the bond numbers in these compounds, a comparison of these lengths indicates the Hf-Hf bonds in HfN probably contain one more electron than do those bonds in HfC. If the calculations of Gibson *et al.* and Erginsoy *et al.* qualitatively describe the local environment of the decaying Hf nuclei following Coulomb excitation, then local vacancies should be produced in HfC and HfN. Following Rundle, one expects the HfN lattice to distort less than the HfC lattice with the removal of a nonmetal atom, since the Hf-Hf bonds are more influential in HfN and therefore tend to retain the lattice symmetry.

Similarly, the higher melting temperature of HfC is indicative of the more dominant role which the Hf-C bonds play in HfC compared to the Hf-N bonds in HfN. The creation of vacancies in HfC might thus be expected to cause greater lattice distortions than similar vacancy configurations in HfN. In general, one would expect the largest distortions to occur in crystals having the strongest metal-nonmetal bonds, i.e., the highest melting temperature, and the least influential metal-metal bonds, i.e., the largest metal-metal separations.

With the exception of HfB_2, all the compounds exhibited different hyperfine interaction energies as targets than as absorbers. A graphical comparison of the hyperfine interaction energies as reported in the literature and observed in these experiments is shown in Fig. 9. As targets all of the compounds exhibited hyperfine linewidths greater than about 1.9 times $2\Gamma_{nat}$. Since it has been shown that the effective absorber thickness of the 77-mg/cm^2 HfC absorber is less than $t=5$ which implies an absorber broadening less than 1.7, it is concluded that recoil radiation damage occurred in all of the targets. In this context, the observation of anomalously broad hyperfine linewidths probably correspond to unresolved structure from more than one vacancy configuration. Evidently, Hf metal, HfB_2, and HfO_2 tend to retain their lattice symmetry since these compounds showed smaller lattice distortions than HfC and HfN.

Hafnium metal, boride, and oxide are not part of the class of compounds to which Rundle's model is applicable. The metal and boride have hexagonal crystal structures. The oxide has a monoclinic crystal structure and is clearly ionic. Since these compounds are not cubic, they have hyperfine interactions even when no lattice damage is present. Significant differences in the hyperfine interaction energy between damaged and undamaged lattices were not observed in the boride and metal. The broad lines required to fit the data, however, indicate that damage has occurred. The anomalous hyperfine interactions in the oxide target probably reflect local-charge imbalances.

VI. CONCLUSIONS

The Mössbauer effect has been observed following the Coulomb excitation of Hf nuclei located in Hf metal, HfB_2, HfC, HfN, and HfO_2. The resulting Mössbauer spectra were found to be anomalous in that: (a) With the exception of HfB_2, hyperfine interaction energies were found to be larger when a compound was used as a target than when the compound was used as an absorber. (b) In most cases the widths of the hyperfine Mössbauer lines required to obtain good fits to the data were at least 50% greater than could be accounted for from lifetime and absorber thickness considerations.

By assuming specific values for the hyperfine interactions parameters of each compound when used as a target, all target-absorber combinations were found to be consistent. With the exception of HfB_2, the interaction parameters for the compounds when used as absorbers were found to be consistent with those reported in the literature. The value obtained for the hyperfine interaction energy in HfB_2 was found to be $(10.6\pm4.5)\%$ larger than that reported by Snyder *et al.*[15]

It is concluded that the anomalous hyperfine interactions in the targets result from radiation damage associated with the stopping of the recoil excited Hf nuclei, since (a) radiation damage resulting from the incident α particles can be ruled out, and (b) published computer calculations indicate that the recoil Hf nuclei probably stop at lattice sites, producing local vacancies. Observed target recoilless fractions are consistent with these conclusions. The broad lines required to fit the data are interpreted as unresolved structure in the targets, resulting from more than one lattice vacancy configuration.

It is concluded that the degree to which local vacancies effect the electric field gradient at the Hf nuclei is related to the particular bonding properties of each compound. A bonding model proposed by Rundle to explain the physical properties of a class of compounds including HfC and HfN was found to be consistent with the results of these experiments.

The observations of recoil radiation damage following Coulomb excitation has a number of implications. Magnetic dipole and electric quadrupole moments have been determined via the Mössbauer effect following Coulomb excitation in a number of instances. Unless it can be clearly demonstrated that recoil radiation damage did not occur, such measurements are now open to question. It is also apparent that the Mössbauer effect following Coulomb excitation can usefully be used to study radiation damage. When other sources of radiation damage can be ruled out, Mössbauer-effect observations have the particular advantage over the other techniques in that the probe nuclei themselves are responsible for the damage.

In addition, it was found that reduction in target recoilless fraction from beam current heating can be significant. Reduced recoilless fractions are therefore not necessarily a good indication of radiation damage.

ACKNOWLEDGMENTS

The authors would like to thank Dr. E. David Cater and Dr. N. C. Baenziger of the Department of Chemistry for assistance in preparing the enriched HfC targets and in taking the Debye-Scherrer powder patterns, and also to acknowledge their informative discussions. The continued interest of Professor R. R. Carlson and Professor J. W. Schweitzer is gratefully acknowledged. The authors would also like to thank J. B. Jeffries for his assistance in many phases of these experiments, and G. W. Hartnell and K. A. Murphy for their cooperation and assistance.